SUA Slovak University of Agriculture in Nitra
SUA·FE Faculty of Engineering
DOI: 10.2478/ata-2026-0004

Acta Technologica Agriculturae 1
Nitra, Slovaca Universitas Agriculturae Nitriae, 2026, pp. 27–34

COMPARATIVE STUDY OF NIR-BASED MACHINE LEARNING FOR PREDICTING SOIL NUTRIENTS IN INDONESIAN FARMLANDS

Adnan ADNAN[1], Taufik Iqbal RAMDHANI[2, 3]*, Yaya SURYANA[1], Abdul AZIZ[1], Taslim ROCHMADI[1], Amrullah KAMARUDDIN[1], Ninon Nurul FAIZA[4]

[1]National Research and Innovation Agency, Research Organisation for Energy and Manufacture, Research Centre for Sustainable Production System and Life Cycle Assessment, Tangerang Selatan, Indonesia, adna002@brin.go.id, yaya002@brin.go.id, abdu002@brin.go.id, tasl001@brin.go.id, amru001@brin.go.id
[2]National Research and Innovation Agency, Research Organisation for Electronics and Informatics, Research Centre for Artificial Intelligence and Cyber Security, Bandung, Indonesia
[3]Universitas Indonesia, Faculty of Engineering, Department of Electrical Engineering, Depok, Indonesia
[4]National Research and Innovation Agency, Centre for Data and Information, Jakarta, Indonesia, nino003@brin.go.id
*correspondence: tauf022@brin.go.id

This study evaluates the efficacy of machine learning models for predicting soil nitrogen (N), phosphorus (P), and potassium (K) concentrations from near-infrared (NIR) spectral data (750–2499 nm). A comparative analysis was conducted on models from three distinct categories: linear-based, non-linear kernel-based, and neural network-based, using data from 145 soil samples collected across four Indonesian provinces. Regularised linear modelling performed best: Ridge Regression achieved R^2/MAE of 0.999/0.00005% for N-Total, 0.868/0.01408% for P-Total, and 0.763/0.01239% for K-Total. The non-linear SVR delivered moderate fit (R^2 = 0.821 for N-Total) but produced the lowest MAE for K (0.00829%) at lower explained variance (R^2 = 0.419). Neural network-based models underperformed the linear baselines. This study demonstrates that, for this dataset, a simpler regularised linear model outperformed more complex architectures, underscoring the critical role of rigorous model selection in developing accurate spectroscopic tools for precision agriculture. Future research could explore hybrid or ensemble methods to combine the strengths of different model types, potentially improving prediction accuracy and robustness.

Keywords: spectral data; soil nutrient; PLSR; SVR; ElasticNet; LassoNet; Ridge; TabNeT

Soil nutrient assessment is an essential aspect of agricultural management, directly influencing crop yield and the ecological sustainability of farming practices. Traditional soil testing methods, although effective, are often labour-intensive, costly, and time-consuming. These methods typically involve chemical analysis in laboratories, which can delay decision-making processes in dynamic farming environments (Farrar et al., 2023; Niu et al., 2023). As global agricultural demands increase and environmental concerns grow, there is a pressing need for rapid, accurate, and non-invasive soil testing techniques.

In response to these challenges, recent technological advances have facilitated spectral analysis as a promising alternative for assessing soil properties. Spectral analysis involves measuring the interaction between electromagnetic radiation and soil components, offering a rapid assessment of various soil attributes, including nutrient content (Liu et al., 2021; Sun et al., 2022). Reflectance spectroscopy, in particular, has been recognised for its potential to estimate soil organic matter (SOM) and other critical soil nutrients effectively (Reis et al., 2021; Sorenson et al., 2020).

Over the past five to six years, vis-NIR and NIR studies have consistently reported strong predictability for total nitrogen, with validation R^2 commonly in the 0.80–0.95 range when models are properly regularised or tuned; corresponding errors for N typically fall in the 0.05–0.15 g·kg^{-1} band for well-controlled laboratory spectra (Oberholzer et al., 2024). Phosphorus and potassium remain more challenging because their spectral responses are largely indirect. Recent works generally report P $R^2 \approx 0.60–0.80$ and K $R^2 \approx 0.50–0.80$ under careful preprocessing and variable selection, with MAE values for P and K on the order of single to tens of mg·kg^{-1} depending on whether totals or plant-available fractions are modelled, the wavelength domain, and the breadth of the calibration set (Guo et al., 2021). When very large spectral libraries or hybrid feature pipelines are available, deep and ensemble methods can push these figures higher; however, on small-to-moderate datasets, regularised linear or latent-variable models frequently deliver equal or better generalisation (Munawar et al., 2024; Ng et al., 2020).

However, interpreting spectral data to accurately determine soil nutrient levels requires sophisticated analytical methods. Traditional methods such as partial least squares regression (PLSR) have been widely used, but recent studies indicate that machine learning (ML) techniques can significantly enhance prediction accuracy and reliability (Chabrillat et al., 2019; Hu et al., 2018). Machine learning models, particularly those employing deep learning algorithms, can handle large datasets and uncover complex

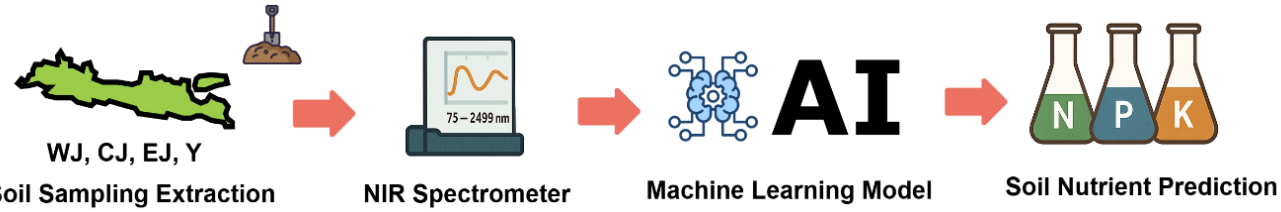

Fig. 1 Research objective

patterns that are not easily discernible through conventional methods (Padarian et al., 2019; Zhong et al., 2021).

The study's primary objective is to predict the concentrations of N, P, and K shown in Fig. 1 using a range of machine learning models, categorised into three distinct groups: linear regression models, deep neural network models, and non-linear machine learning models. The choice of Indonesian provinces as study locations – East Java, West Java, Central Java, and Jogjakarta – provides a diverse dataset reflective of different soil types and agricultural practices prevalent in tropical regions. Indonesia's varied climatic conditions and soil characteristics make it an ideal case for testing and validating the generalisability of ML models. Spectral data ranging from 750 to 2499 nm help cover a broad spectrum of soil characteristics, enhancing the generalisability and applicability of the developed ML models. The models include PLSR, ElasticNet, LassoNet, ridge regression, a deep neural network (DNN), TabNetRegressor, and support vector regression (SVR). Each model is subjected to hyperparameter tuning to optimise performance and ensure the most accurate predictions. While deep neural networks and other complex models are often expected to excel in handling high-dimensional data, preliminary results indicated that simpler linear models like ridge regression could offer superior performance in certain contexts. This observation underscores the importance of careful model selection and highlights the potential pitfalls of assuming that more complex models will always yield better results (Singha et al., 2023; Xu et al., 2024).

This paper is structured as follows. Section 2 details the materials and methods, including the data collection protocol, preprocessing steps, the construction of the various machine learning models, and the evaluation metrics used. Section 3 presents the results and discussion, beginning with an analysis of the collected data and followed by a comparative evaluation of the predictive performance of each model. Finally, Section 4 concludes the paper by summarising the key findings and offering directions for future research.

Material and methods

This study employs a comparative analysis approach to evaluate the effectiveness of different machine learning algorithms. The methodology encompasses several stages: data collection, preprocessing, model training, validation, and performance evaluation. The data gathered will be pre-processed before being supplied as training data for different types of models that can be compared to the performance of each model.

Data collection

The development of predictive machine learning models required a robust and varied dataset, the construction of which was achieved through a multi-stage data collection protocol. This protocol was designed to ensure data quality, consistency, and representativeness. It encompassed four primary stages depicted in Fig. 2.

Study area and site selection

The study was situated on the island of Java, Indonesia, a region selected for its pronounced diversity in agricultural practices, soil typologies, and environmental conditions, thereby providing an ideal context for evaluating the generalisability of the resulting predictive models. A purposive sampling strategy was employed to ensure the inclusion of a wide spectrum of land characteristics. This strategy aimed to capture maximal variance in soil properties, a critical prerequisite for developing a widely applicable soil fertility model.

Site selection was conducted in consultation with the regional Department of Agriculture, with final sampling points identified by local agricultural extension specialists and farmers. This collaborative approach facilitated access to sites representing a comprehensive range of variables, including geographic distribution (western, central, and eastern Java), land type (wet and dry), vegetation (varied crops and growth phases), and topography (lowlands and highlands). A total of 145 distinct locations were sampled across the specified provinces.

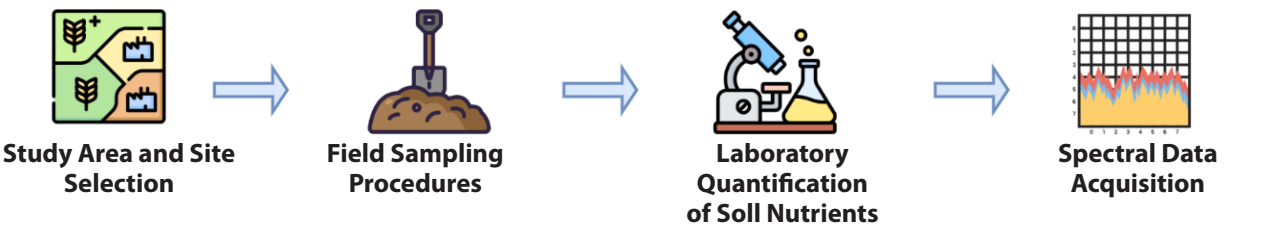

Fig. 2 Data collection stages

Field sampling procedures

To ensure each sample was representative of its respective location, a composite sampling strategy was adopted. At each of the 145 sites, five sub-samples were collected and combined into a single composite, with the spatial placement of sub-sampling points guided by local agricultural specialists to capture known micro-variability that rigid geometric patterns might miss. Each location covered approximately 2000–10,000 m^2 (up to 1 ha), depending on land conditions; however, plot size was not a design constraint in this study, as the primary objective was to capture soil diversity for database development.

At each sub-sampling point, the soil surface was cleared of grass, stones, and plant residues before excavating a V-shaped hole to a depth of roughly 30 cm using a hoe, supplemented with a crowbar or fork in compacted soils (depicted in Fig. 3). A vertical slice of uniform thickness (≈5 cm) was then taken from the excavation wall. The five sub-samples were thoroughly homogenised in a bucket and on a clean tarpaulin to form the composite sample, from which 2–6 kg was retained, sealed in double zip-lock bags, and labelled with a unique ID and comprehensive metadata. To prevent cross-contamination, all tools were cleaned after processing each composite sample. To maximise environmental and pedological heterogeneity, sampling spanned four provinces and eight regencies across Java, covering the island's western, central, and eastern regions and encompassing diverse agricultural ecosystems, including lowlands and highlands as well as rice paddies and dryland fields. This geographic and land-use spread was selected to enrich the spectral and chemical variability captured by the dataset and thereby strengthen downstream model development and validation.

Fig. 3 Soil sampling technique

Laboratory quantification of soil nutrients

Following field collection, laboratory analyses were performed to quantify the chemical properties of the soil samples. Aliquots of approximately 1 kg from each composite sample were used for these analyses. Key soil fertility and health indicators were measured using a suite of established analytical methods. Soil pH was measured in a 1 : 5 soil-to-water (H_2O) solution, and organic carbon (C-organic, %) was assessed using the Walkey & Black method. Total nitrogen (N-total, %) was determined by the Kjeldahl method. Total phosphorus (P-total, ppm) was measured by spectrophotometry and total potassium (K-total, ppm) by flame photometry, with both analyses following an HNO_3 : $HClO_4$ digestion. Additionally, available nutrient levels were quantified; available phosphorus (P, ppm) was determined using the Bray I extraction method, while available potassium (K, cmol(+).kg) was measured after extraction with N NH_4OAc at pH 7.0. Finally, nitrate (N-NO_3, ppm) and ammonium (N-NH_4, ppm) concentrations were quantified using titrimetry, and the gravimetric method was employed to determine the water content percentage.

Spectral data acquisition

Prior to spectral acquisition, all soil samples underwent standardised preparation to minimise signal interference and ensure data consistency. Samples were first air-dried for approximately two weeks to reduce moisture content, as water absorption bands are known to interfere significantly with NIR spectra. Subsequently, the dried soil was ground with a mortar and sieved (60–80 mesh) to achieve a uniform, fine particle size, thereby reducing variability from light scattering effects (depicted in Fig. 4).

Fig. 4 Drying and grinding soil samples

Spectral data were acquired using an Attenuated Total Reflectance (ATR) module on a Bruker Tensor 27 FTIR spectrometer in the laboratory. The instrument was equipped with a liquid nitrogen-cooled MCT detector and set to a resolution of 1 cm^{-1}. For each sample, a background spectrum was collected from an empty well to compensate for ambient atmospheric conditions. To account for intra-sample heterogeneity and variations in packing density, four scans were performed per sample well, and the resulting spectra were averaged to produce a final, representative spectrum. The final data, recorded as absorbance across the 750 to 2499 nm range, were exported in .csv format for subsequent model development.

Data preprocessing

Data preparation is a critical step in machine learning, ensuring the dataset is clean, consistent, and ready for modelling. In this study, we performed several preprocessing steps to prepare the dataset for analysis, addressing missing values, encoding categorical variables, and ensuring data consistency. First, we checked for missing values and removed rows with incomplete entries to avoid bias and maintain integrity in downstream modelling. Next, we handled categorical variables by mapping and encoding them into numerical representations; where

applicable, string fields were converted to categorical types and expanded into binary indicators so that the algorithms could interpret them effectively.

After preprocessing, the dataset was split into training (70%) and test (30%) subsets (Renard et al. 2020). Hyperparameter optimisation was conducted exclusively on the validation set with Optuna's Tree-structured Parzen Estimator (TPE) sampler, while the test set was held out for a single, final performance assessment (Cudennec, 2025; Rong et al., 2021). To prevent information leakage, all learned preprocessing operations were estimated on the training data only and then applied unchanged to the validation and test sets. This protocol ensures a fair comparison across models and provides reliable estimates of generalisation performance for predicting soil properties from NIR spectra.

Model construction

We selected a diverse suite of models of PLSR, Ridge Regression, ElasticNet, LassoNet, SVR, DNN, and TabNetRegressor to span linear latent-variable methods, regularised linear estimators, kernel approaches, and modern neural or tabular architectures, thereby covering the bias-variance spectrum, addressing severe spectral collinearity, and balancing predictive accuracy with interpretability in high-dimensional NIR settings. All models were used as off-the-shelf implementations without architectural modification, and their hyperparameters were optimised with Optuna using TPE with 50 tries for each model to ensure a fair, capacity-matched comparison on the same dataset.

PLSR projects spectra and responses onto covariance-maximising latent components, producing stable estimates when predictors are highly collinear and $p \gg n$ (Sadergaski et al., 2023). Ridge Regression applies L2 shrinkage to stabilise coefficients under correlated wavelengths and serves as a strong linear baseline (Wang et al., 2022). ElasticNet combines L1 and L2 penalties to yield sparse yet stable solutions that accommodate groups of correlated spectral features, enabling embedded feature selection (Rauschenberg et al., 2021). LassoNet enforces global feature sparsity through a hierarchical L1 constraint while retaining non-linear representation capacity, bridging linear sparsity with neural modelling (Yeo et al., 2025). SVR adopts an ε-insensitive loss and kernel mappings to construct robust non-linear functions in high-dimensional feature spaces, performing reliably with moderate sample sizes (Wei and He, 2023). The DNN captures complex, non-linear spectra-nutrient relationships through a multilayer perceptron trained by backpropagation under explicit regularisation (Debus et al., 2021). TabNetRegressor introduces sequential attention with sparse feature masks tailored to tabular inputs, focusing the model on informative wavelength regions while preserving localised interpretability (McDonnell, 2023). Collectively, this design tests how far linear baselines can go when collinearity is handled explicitly, whether sparsity with non-linearity improves fit while highlighting salient wavelengths, and the extent of gains achievable from high-capacity non-linear learners under continuous tuning.

Model evaluation

The performance of the models was evaluated using the *R*-squared (R^2) and mean absolute error (MAE) percentage. R^2, also known as the coefficient of determination, measures the proportion of the variance in the dependent variable that is predictable from the independent variables (Chicco et al., 2021). It provides an indication of how well the model fits the data. R^2 values range from 0 to 1, where a value closer to 1 indicates a model that explains a high proportion of the variance in the dependent variable, while a value closer to 0 indicates a model that explains very little variance (Chicco et al., 2021). In some cases, R^2 can be negative, indicating that the model performs worse than a simple mean of the data. MAE is being used to provide a clear measure of each model's predictive capability, allowing for a direct comparison between the linear regression model and the DNN in terms of their ability to predict soil nutrient content from spectral data (Hodson, 2022).

Results and discussion

Data analysis

145 samples were collected in four Indonesian provinces: East Java, West Java, Central Java, and Jogjakarta, providing an insightful perspective on indicating soil nutrient properties. Soils in Indonesia are predominantly formed under tropical climates, which are characterised by high temperatures and heavy rainfall. Figure 5 shows the absorbance and transmittance spectrum of NIR light by the soil samples across the wavelength range of 750 to 2499 nm.

In diffuse reflectance spectroscopy of soils, raw reflectance R is routinely transformed to pseudo-absorbance $A = \log(1/R)$ because the logarithmic mapping approximates Beer-Lambert behaviour, improves linearity with concentration, and stabilises variance for multivariate calibration. Recent soil spectroscopy studies and transfer-learning workflows adopt this transform explicitly and report stronger correlations between soil properties than with raw R (Munnaf and Mouazen, 2023). Within the 750–2499 nm window, the absorbance spectra of mineral soils exhibit diagnostic features: strong O–H water bands near 1400 and 1900–1950 nm, and combination bands linked to clay lattice OH groups (Al–OH, Mg–OH) around 2200–2350 nm; these assignments are consistently reported in recent laboratory and field evaluations and in radiative-transfer analyses of soil spectra (Wangeci et al., 2024). In our context, plotting each of the 145 samples as individual absorbance curves over 750–2499 nm preserves sample-level structure across these moisture and clay-related regions, which is essential for chemometric and machine-learning calibration.

Transmittance provides the complementary view of optical throughput but is nonlinearly related to concentration, converting to absorbance yields the linear optical density used in quantitative analysis. Contemporary optical diagnostics continue to ground this relation in Beer-Lambert physics, while soil vis-NIR method papers increasingly emphasise working in absorbance space for regression (Zhang et al., 2022). When transmittance is available, as in our dataset, displaying all 145 transmittance

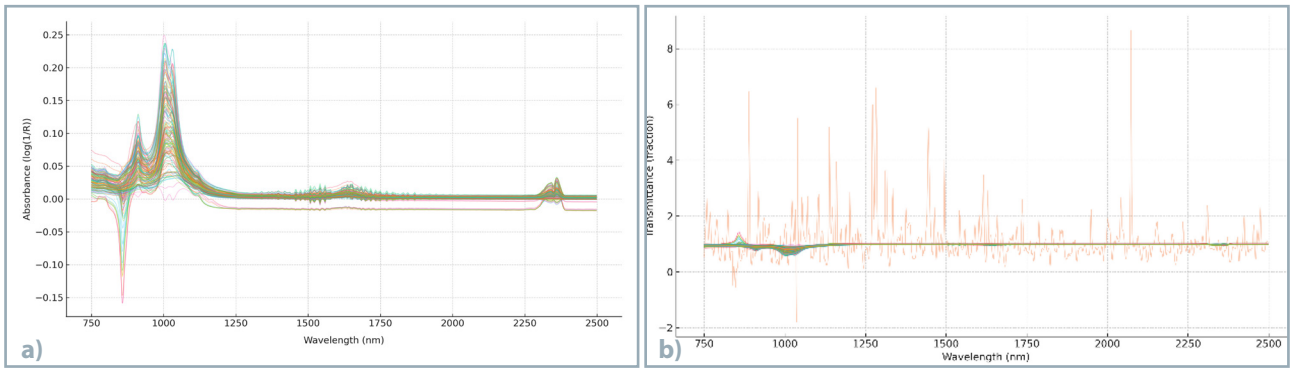

Fig. 5 (a) Absorbance spectra; (b) Transmittance spectra of NIR wavelengths from soil samples

curves across 750–2499 nm complements the absorbance view by revealing sample-to-sample differences in overall attenuation through the water- and clay-active bands, which recent studies identify as the most information-rich intervals for soil characterisation (Deng et al., 2025).

Figure 6 compares key soil nutrients of total N, total P, and total K across the provinces of West Java (JB), East Java (JI), Central Java (JT), and Yogyakarta (YO). In terms of total P, JI has the highest average of total P at 1045, indicating a relatively higher phosphorus content compared to other provinces. JB also shows a substantial phosphorus level, with an average of 826, while JT has moderate phosphorus content, with an average of 753. YO shows the lowest phosphorus content, with an average of 436, potentially indicating a need for phosphorus fertilisation. The findings of total K show that JT and JB have similar levels of potassium with averages around 629 and 621, respectively. Lower potassium levels, with an average of 354, is shown in JT. The lowest potassium content, with an average of 295, suggests possible potassium limitations in the soil of YO. Overall, JT and JB generally show higher levels of key nutrients, indicating better soil fertility compared to YO and JT. YO consistently has the lowest levels of all the three nutrients, highlighting the potential need for nutrient management interventions in this province. JT has moderate fertility but lower potassium levels than the other provinces.

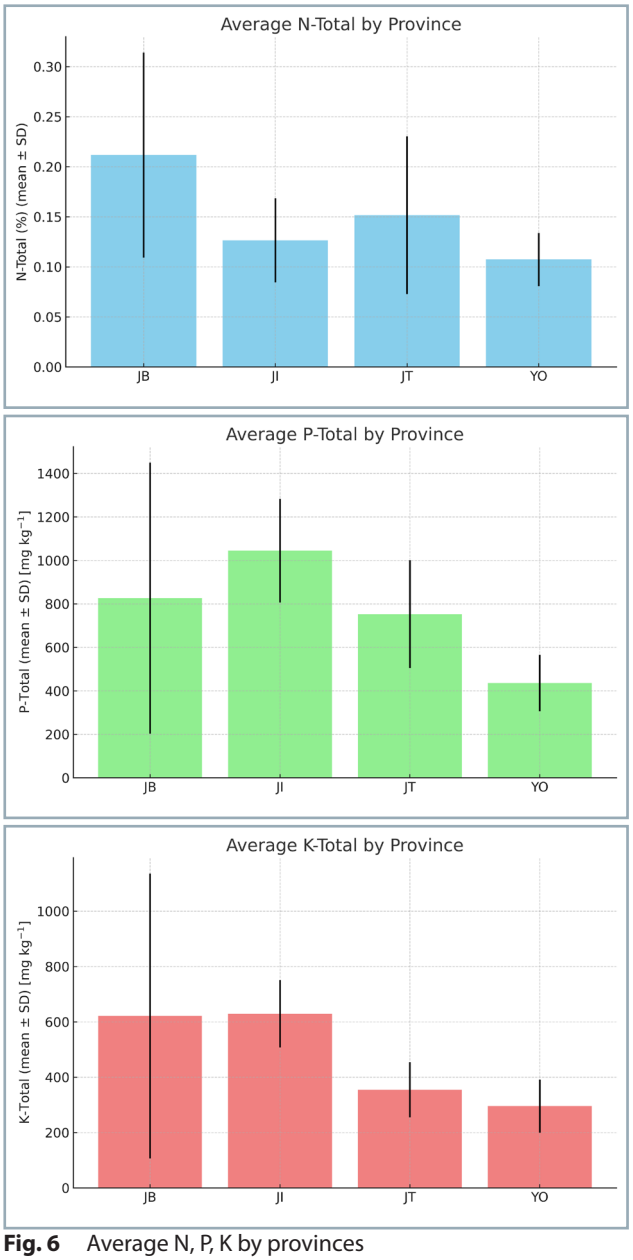

Fig. 6 Average N, P, K by provinces

Model results

The comparative analysis of the linear regression-based models, DNN models, and non-linear-based models depicted in Fig. 7 revealed distinct performance differences across the three primary soil nutrients: nitrogen (N), phosphorus (P), and potassium (K). We provide the simple linear regression task to handle the diverse dataset of Indonesian soil. In comparison, the deep neural network architecture constructed to observe the more complex model is favourable to predicting the soil nutrient properties of the ATR data. We offer automatic hyperparameter tuning using Optuna with 50 tries for all models.

Table 1 presents a comparative analysis of the performance of various machine learning models in predicting soil nutrient concentrations. Across nutrients, the results show a clear advantage for regularised linear modelling on this dataset. For total N, Ridge achieved 0.999 for R^2 and 0.00005% for MAE, surpassing typical recent benchmarks. On visible and shortwave near-infrared

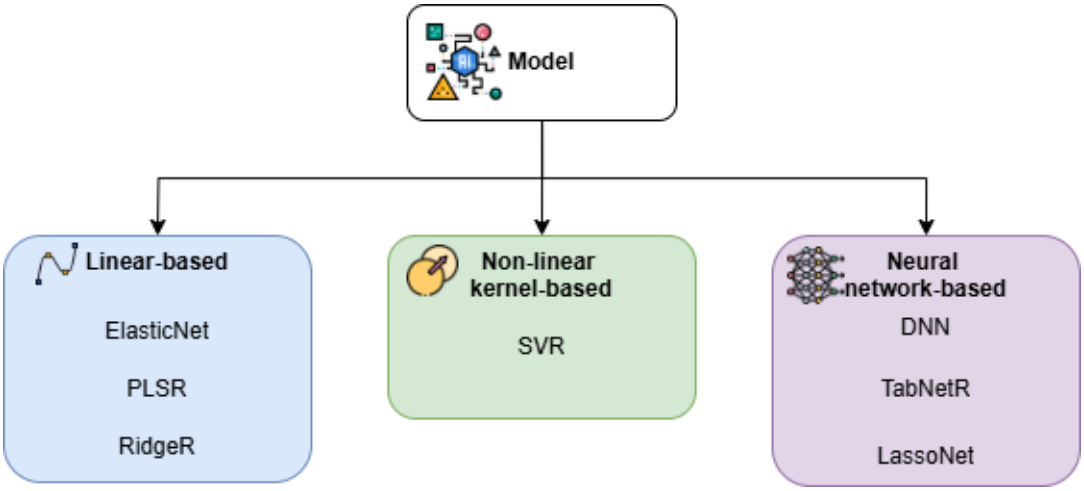

Fig. 7 Model categories

spectroscopy (Vis/SW-NIR) with 350–1070 nm, Qi et al. (2025) reported R^2 = 0.972 for total nitrogen with low error using an optimised partial least square with back-propagation neural network (PLS-BPNN), confirming that N is highly learnable from NIR features linked to organic matter signals. In contrast, Tan et al. (2022) reported workflows on laboratory NIR often attain $R^2 \approx 0.80–0.85$ for test sets on 143 samples, R^2 = 0.83, well below our linear baseline. Deep models can reach high N accuracy when data are abundant, attention-augmented bidirectional gated recurrent units (BiGRU) on hyperspectral reflectance proposed by H. Wang et al. (2023) reported validation R^2 = 0.907 for N, though still short of our Ridge fit. For total P, Ridge reached R^2 = 0.868 with MAE = 0.01408%, exceeding several recent Vis-NIR reports that typically show moderate predictability. For example, El-Mejjaouy et al. (2025) obtained R^2 = 0.74 with RMSE = 14.09 mg kg^{-1} for available P using Vis-NIRS plus UAV features, while the attention-BiGRU of (H. Wang et al., 2023) study achieved R^2 = 0.921 for P on its dataset. For total K, the picture is mixed, Ridge delivered the highest explained variance (R^2 = 0.763; MAE = 0.01239%), whereas SVR minimised average error (MAE = 0.00829%) at lower explained variance (R^2 = 0.419), evidencing an accuracy-explainability trade-off. Recent potassium studies often report weaker fits than for N. An Fourier-transform infrared with partial least squares regression (FTIR–PLSR) workflow, studied by W. Wang et al. (2023) on 145 soils, reported R^2 = 0.49 with MAE = 16.82 mg kg^{-1} for available K, while a VIS-NIR boosting approach of Jin et al. (2020), after aggressive preprocessing and task stratification, reported test R^2 >0.90 for available K, illustrating that algorithm pretreatment choices and K definition (available vs total) strongly affect attainable accuracy.

These comparisons position our Ridge models at the upper range of recent Vis/Vis-NIR studies for N and P and competitive for K. The literature shows that high R^2 for N is common with well-regularised or optimised models, while P typically attains $R^2 \approx 0.7–0.8$, unless auxiliary structure such as attention mechanisms and feature fusion, lifts performance. Our R^2 = 0.868 for P exceeds those mid-range results and approaches the best deep-learning reports (El-Mejjaouy et al., 2025; H. Wang et al., 2023; Qi et al., 2025). For K, our findings align with recent evidence that K's spectral signature is largely indirect. Linear models can rank variability well with higher R^2, whereas kernel methods can compress residuals with lower MAE without capturing the full variance. The external results of R^2 = 0.49; MAE = 16.82 mg·kg^{-1} for FTIR–PLSR, and R^2 >0.90 for VIS-NIR boosting under curated settings underscore that attainable accuracy hinges on wavelength domain, pretreatment and feature selection, K fraction (total vs available), and model bias-variance control (W. Wang et al., 2023; Jin et al., 2020).

Table 1 Performance comparison

Model	Accuracy					
	R^2			MAE (%)		
	N	P	K	N	P	K
PLSR	0.862	0.767	-0.545	0.0363	0.02043	0.01384
TabNetR	0.125	0.197	0.464	0.055	0.02059	0.01909
ElasticNet	0.781	0.85	-0.508	0.0361	0.01911	0.01526
LassoNet	0.793	0.846	-0.383	0.0349	0.01892	0.01454
SVR	0.821	0.491	0.419	0.0305	0.02498	0.00829
DNN	-0.27	0.385	0.517	0.0607	0.0188	0.01375
Ridge	0.999	0.868	0.763	0.00005	0.01408	0.01239

Conclusion

This study demonstrates that near-infrared (750–2499 nm) spectroscopy combined with machine learning enables accurate, rapid prediction of soil macronutrients across diverse tropical soils. Using 145 composite samples from four Indonesian provinces and a standardised preprocessing-tuning protocol, regularised linear modelling provided the strongest and most stable performance. Ridge regression achieved near-perfect prediction for total N (R^2 = 0.999; MAE = 0.00005%), and delivered the highest accuracy for total P (R^2 = 0.868; MAE = 0.01408%) and strong performance for total K (R^2 = 0.763; MAE = 0.01239%). ElasticNet and LassoNet remained competitive for N and P (R^2 ≈ 0.78–0.85; MAE ≈ 0.035–0.019%), whereas PLSR ranked mid-tier for N and P and failed on K (negative R^2). For K, a metric trade-off emerged: SVR minimised absolute error (MAE = 0.00829%) while explaining less variance (R^2 = 0.419). DNN and TabNet underperformed across nutrients despite hyperparameter optimisation, confirming that with n = 145 and dominantly linear spectrum-chemistry relations, well-regularised linear baselines generalise better than high-capacity architectures.

These findings establish clear modelling guidance for operational soil diagnostics with NIR. For N and P, regularised linear models should be used as defaults because they exploit the broad, collinear spectral structure linked to organic matter and clay-associated proxies, delivering high accuracy with transparent behaviour and low computational cost. For K, model choice must follow the decision metric: use Ridge when ranking or explained variance matters, and SVR when minimising average error is critical. The pipeline-field compositing, ATR-based spectra, split discipline, and Optuna-TPE tuning, provides a reproducible template for rapid nutrient mapping.

The study is limited by the sample size (n = 145), single-instrument laboratory spectra, and a focus on total N, P, and K rather than plant-available fractions. Next steps are: expand and diversify the calibration library, perform external cross-region validation, incorporate variable-selection or hybrid/ensemble designs, quantify and report prediction uncertainty, evaluate multi-sensor fusion, and calibration-transfer/domain-adaptation strategies. Implementing these steps will scale the demonstrated accuracy to broader agroecosystems and strengthen decision support for precision nutrient management.

Acknowledgement

This research is fully supported by Research and Innovation for Advanced Indonesia (RIIM), B-1112/III.3.7/OT.00.00/2/2024. The authors fully acknowledged the National Research and Innovation Agency of Indonesia (BRIN) and Indonesia Endowment Fund for Education Agency (LPDP) for the approved fund which makes this important research viable and effective.

References

Chabrillat, S., Ben-Dor, E., Cierniewski, J., Gomez, C., Schmid, T., Van Wesemael, B., 2019. Imaging spectroscopy for soil mapping and monitoring. Surveys in Geophysics 40(3), 361–399. https://doi.org/10.1007/s10712-019-09524-0

Chicco, D., Warrens, M.J., Jurman, G., 2021. The coefficient of determination R-squared is more informative than SMAPE, MAE, MAPE, MSE and RMSE in regression analysis evaluation. PeerJ Computer Science 7, e623. https://doi.org/10.7717/peerj-cs.623

Cudennec, L., 2025. Scaling Up Optuna: P2P distributed hyperparameters optimization. Concurrency and Computation: Practice and Experience 37(4–5), e70008. https://doi.org/10.1002/cpe.70008

Debus, B., Parastar, H., Harrington, P., Kirsanov, D., 2021. Deep learning in analytical chemistry. TrAC Trends in Analytical Chemistry 145, 116459. https://doi.org/10.1016/j.trac.2021.116459

Deng, Y., Kong, K., Zhang, X., Cao, J., Liu, J., Bao, W., Ma, R., Xie, W., Zhang, B., 2025. Strategies for the efficient estimation of multi-scale soil properties from spectral degradation through Vis-NIR spectroscopy. Infrared Physics and Technology 150, 105994. https://doi.org/10.1016/j.infrared.2025.105994

El-Mejjaouy, Y., Bastin, J.-F., Baeten, V., Meersmans, J., Oukarroum, A., Dumont, B., Mercatoris, B., 2025. Spectral and textural features for predicting soil phosphorus using Vis-NIR point data and multispectral UAV imagery: A case study from a long-term experiment. Journal of Plant Nutrition and Soil Science. https://doi.org/10.1002/jpln.12012

Farrar, M.B., Wallace, H.M., Tahmasbian, I., Yule, C.M., Dunn, P.K., Hosseini Bai, S.HHHHhhhH., 2023. Rapid assessment of soil carbon and nutrients following application of organic amendments. CATENA 223, 106928. https://doi.org/10.1016/J.CATENA.2023.106928

Guo, P., Li, T., Gao, H., Chen, X., Cui, Y., Huang, Y., 2021. Evaluating calibration and spectral variable selection methods for predicting three soil nutrients using VIS-NIR spectroscopy. Remote Sensing 13(19), 4000. https://doi.org/10.3390/rs13194000

Hodson, T.O., 2022. Root-mean-square error (RMSE) or mean absolute error (MAE): when to use them or not. Geoscientific Model Development 15(14), 5481–5487. https://doi.org/10.5194/gmd-15-5481-2022

Hu, L., Yin, C., Ma, S., Liu, Z., 2018. Rapid detection of three quality parameters and classification of wine based on Vis-NIR spectroscopy with wavelength selection by ACO and CARS algorithms. Spectrochimica Acta Part A: Molecular and Biomolecular Spectroscopy 205, 574–581. https://doi.org/10.1016/J.SAA.2018.07.054

Jin, X., Li, S., Zhang, W., Zhu, J., Sun, J., 2020. Prediction of soil-available potassium content with visible near-infrared ray spectroscopy of different pretreatment transformations by the boosting algorithms. Applied Sciences 10(4), 1520. https://doi.org/10.3390/app10041520

Liu, J., Dong, Z., Xia, J., Wang, H., Meng, T., Zhang, R., Han, J., Wang, N., Xie, J., 2021. Estimation of soil organic matter content based on CARS algorithm coupled with random forest. Spectrochimica Acta Part A: Molecular and Biomolecular Spectroscopy 258, 119823. https://doi.org/10.1016/J.SAA.2021.119823

McDonnell, K., Murphy, F., Sheehan, B., Masello, L., Castignani, G., 2023. Deep learning in insurance: Accuracy and model interpretability using TabNet. Expert Systems with Applications 217, 119543. https://doi.org/10.1016/j.eswa.2023.119543

Munawar, A.A., Kusumiyati, Andasuryani, Yusmanizar, Adrizal, 2024. Near infrared technology coupled with different spectra correction

approaches for fast and non-destructive prediction of chlorogenic acid on intact coffee beans. Acta Technologica Agriculturae 27(1), 23–29. https://doi.org/10.2478/ata-2024-0004

Munnaf, M.A., Mouazen, A.M., 2023. Spectra transfer based learning for predicting and classifying soil texture with short-ranged Vis-NIRS sensor. Soil and Tillage Research 225, 105545. https://doi.org/10.1016/j.still.2022.105545

Ng, W., Minasny, B., de Sousa Mendes, W., Melo Demattê, J.A., 2020. The influence of training sample size on the accuracy of deep learning models for the prediction of soil properties with near-infrared spectroscopy data. Soil 6(2), 565–578. https://doi.org/10.5194/soil-6-565-2020

Niu, Z., Shi, L., Qiao, H., Xu, X., Wang, W., Ma, X., Zhang, J., 2023. Construction of a hyperspectral estimation model for total nitrogen content in Shajiang black soil. Journal of Plant Nutrition and Soil Science 186(2), 196–208. https://doi.org/10.1002/jpln.202100332

Oberholzer, S., Summerauer, L., Steffens, M., Ifejika Speranza, C., 2024. Best performances of visible-near-infrared models in soils with little carbonate – a field study in Switzerland. Soil 10(1), 231–249. https://doi.org/10.5194/soil-10-231-2024

Padarian, J., Minasny, B., McBratney, A.B., 2019. Using deep learning to predict soil properties from regional spectral data. Geoderma Regional 16, e00198. https://doi.org/10.1016/J.GEODRS.2018.E00198

Qi, J., Cheng, P., Zhou, J., Zhang, M., Gao, Q., He, P., Li, L., Muga, F.C., Guo, L., 2025. A novel model for soil organic matter and total nitrogen detection based on visible/shortwave near-infrared spectroscopy. Land 14(2), 239. https://doi.org/10.3390/land14020329

Rauschenberger, A., Glaab, E., van de Wiel, M.A., 2021. Predictive and interpretable models via the stacked elastic net. Bioinformatics 37(14), 2012–2016. https://doi.org/10.1093/bioinformatics/btaa535

Reis, A.S., Rodrigues, M., Alemparte Abrantes dos Santos, G.L., Mayara de Oliveira, K., Furlanetto, R.H., Teixeira Crusiol, L.G., Cezar, E., Nanni, M.R., 2021. Detection of soil organic matter using hyperspectral imaging sensor combined with multivariate regression modeling procedures. Remote Sensing Applications: Society and Environment 22, 100492. https://doi.org/10.1016/J.RSASE.2021.100492

Renard, F., Guedria, S., de Palma, N., Vuillerme, N., 2020. Variability and reproducibility in deep learning for medical image segmentation. Scientific Reports 10(1), 13724. https://doi.org/10.1038/s41598-020-69920-0

Rong, G., Li, K., Su, Y., Tong, Z., Liu, X., Zhang, J., Zhang, Y., Li, T., 2021. Comparison of tree-structured Parzen estimator optimization in three typical neural network models for landslide susceptibility assessment. Remote Sensing 13(22), 4694. https://doi.org/10.3390/rs13224694

Sadergaski, L.R., Irvine, S.B., Andrews, H.B., 2023. Partial least squares, experimental design, and near-infrared spectrophotometry for the remote quantification of nitric acid concentration and temperature. Molecules 28(7), 3224. https://doi.org/10.3390/molecules28073224

Singha, C., Swain, K.C., Sahoo, S., Govind, A., 2023. Prediction of soil nutrients through PLSR and SVMR models by VIs-NIR reflectance spectroscopy. The Egyptian Journal of Remote Sensing and Space Sciences 26(4), 901–918. https://doi.org/10.1016/J.EJRS.2023.10.005

Sorenson, P.T., Quideau, S.A., Rivard, B., Dyck, M., 2020. Distribution mapping of soil profile carbon and nitrogen with laboratory imaging spectroscopy. Geoderma 359, 113982. https://doi.org/10.1016/J.GEODERMA.2019.113982

Sun, W., Liu, S., Zhang, X., Li, Y., 2022. Estimation of soil organic matter content using selected spectral subset of hyperspectral data. Geoderma 409, 115653. https://doi.org/10.1016/J.GEODERMA.2021.115653

Tan, B., You, W., Tian, S., Xiao, T., Wang, M., Zheng, B., Luo, L., 2022. Soil nitrogen content detection based on near-infrared spectroscopy. Sensors 22(20), 8013. https://doi.org/10.3390/s22208013

Wang, H., Zhang, L., Zhao, J., 2023. Application of a fusion attention mechanism-based model combining bidirectional gated recurrent units and recurrent neural networks in soil nutrient content estimation. Agronomy 13(11), 2724. https://doi.org/10.3390/agronomy13112724

Wang, P., Chen, S., Yang, S., 2022. Recent advances on penalized regression models for biological data. Mathematics 10(19), 3695. https://doi.org/10.3390/math10193695

Wang, W., Zhang, Y., Li, Z., Liu, Q., Feng, W., Chen, Y., Jiang, H., Liang, H., Chang, N., 2023. Fourier-transform infrared spectral inversion of soil available potassium content based on different dimensionality reduction algorithms. Agronomy 13(3), 617. https://doi.org/10.3390/agronomy13030617

Wangeci, A., Adén, D., Nikolajsen, T., Greve, M.H., Knadel, M., 2024. Comparing laser-induced breakdown spectroscopy and visible near-infrared spectroscopy for predicting soil properties: A pan-European study. Geoderma 444, 116865. https://doi.org/10.1016/j.geoderma.2024.116865

Wei, J., He, X., 2023. Support vector regression model with variant tolerance. Measurement and Control 56(9–10), 1705–1719. https://doi.org/10.1177/00202940231180620

Xu, S., Zhao, Y., Wang, Y., 2024. Optimizing machine learning models for predicting soil pH and total P in intact soil profiles with visible and near-infrared reflectance (VNIR) spectroscopy. Computers and Electronics in Agriculture 218, 108643. https://doi.org/10.1016/J.COMPAG.2024.108643

Yeo, C., Suh, N., Kim, Y., 2025. Fused LassoNet: Sequential feature selection for spectral data with neural networks. Chemometrics and Intelligent Laboratory Systems 257, 105315. https://doi.org/10.1016/j.chemolab.2024.105315

Zhang, W., Kasun, L.C., Wang, Q.J., Zheng, Y., Lin, Z., 2022. A review of machine learning for near-infrared spectroscopy. Sensors 22(24), 9764. https://doi.org/10.3390/s22249764

Zhong, L., Guo, X., Xu, Z., Ding, M., 2021. Soil properties: Their prediction and feature extraction from the LUCAS spectral library using deep convolutional neural networks. Geoderma 402, 115366. https://doi.org/10.1016/J.GEODERMA.2021.115366